Research Article

Effects of Brownian Motion and Thermophoresis on Magneto Hydrodynamics Stagnation Point of a Nanofluid Boundary Layer Flow on a Stretching Surface with Variable Thickness

Shiva Prasad Rayapole[1], Anand Rao Jakkula[2]

[1,2]*Department of Mathematics, Osmania University, Hyderabad, Telangana.*

ABSTRACT

The paper aims to investigate the properties of Brownian motion and Thermophoresis magento hydro dynamics (MHD) stagnation point of a Nanofluid Boundary layer flow on a stretching surface with inconsistent thickness. The effect of inconsistent thickness is considered and understood that the sheet is defiant. A governing continuity, momentum, angular momentum and heat equations mutually with allied boundary conditions are first abridged to a set of self-similar non-linear united ordinary differential equations by appropriate transformations. These equations are solved numerically by using the Keller Box method. The influence of magnetic parameter M reduced the velocity profile while it increases temperature and nanoparticle volume fraction profiles. It is seen that the boundary layer is formed when $\lambda > 1$ and on other hand an inverted boundary layer is formed when < 1.

Key Words: Stagnation Point, Variable Thickness, MHD, Nanofluid, Thermal Radiation, Stretching Surface

INTRODUCTION

In fluid dynamics, MHD stagnation flow over a stretching sheet has many production applications such as tragedy core cooling system, glass industrialized, sanitization of crude oil, etc. The stagnation-point flow and the flow due to a stretching sheet are equally essential in theoretical and claim point of view. The two-dimensional flow of fluid near a stagnation point was first examined by Hiemenz [1]. Later, Chaim [2] considering the strain-rate of the stagnation-point flow and the stretching rate of the sheet to be identical and found no boundary layer structure near the sheet. Whereas, the performance of stagnation-point flow over stretching vertical under diverse physical aspects was discussed by Ishak A, Nazar R.,[3].Layek et al.,[4], studied the unsteady laminar MHD flow and heat Transfer in the stagnation region. The minority current studies covering similar topics are cited in Refs. [5–16]. Besides stagnation point flow, stretching surfaces

has a ample range of applications in engineering and numerous technical purposes predominantly in metallurgy and polymer industry. For instance, plodding cooling of continuous stretching metal or plastic strips can be mentioned which have various applications in mass production. pointless to say, the final eminence of the product robustly depends on the rate of heat transfer from the stretching surface. Crane [17] is the first to present a identity-analogous solution in the congested analytical form for steady two-dimensional incompressible boundary layer flow caused by the stretching plate whose velocity varies linearly with the distance from a fixed point on the sheet. Following Crane's study, the thermal approach to this crisis was investigated by Carragher and Crane [18]. They tacit that the temperature difference between the sheets and the ambient is comparative to a power of the detachment from the fixed point. Subjecting uniform heat flux boundary condition, Dutta et al. [19] presented the

temperature allocation for a stretching surface in an ambient with different temperatures.

Nanofluid is a fluid containing small particles, called nanoparticles. These fluids are engineered colloidal suspensions of nanoparticles in a base fluidstudied by Buongiorno[20]. The nanoparticles used in nanofluids are classically made of metals, oxides, carbides, or carbon nanotubes. The base fluids used are usually water, ethylene glycol and oilKakac, A. Pramuanjaroenkij& Marga, S.J. Palm[21,22]. Recently, boundary-layer flow of a nanofluid past a stretching sheet was presented by Khan and Pop [23], The natural convective boundary-layer flow of a nanofluid past a vertical plate is presented systematically by Kuznetsov and Nield [24] Vajravelu et al. [25] presented the exhaustive scrutiny of convective heat transfer in the flow of viscous Ag–water and Cu–water nanofluids over a stretching surface. Very recently the boundary layers of an uneven stagnation-point flow in a nanofluid is investigated by Bachok et al. [26], They analyzed that fluid containing solid particles may drastically increase its conductivity. Recently, Bachok et al. coated the boundary layers of an unsteady stagnation-point flow in a nanofluid.

Nanofluids have their foremost applications in heat transfer, as well as microelectronics, fuel cells, pharmaceutical processes, and hybrid-powered engines, domestic refrigerator, chiller, nuclear reactor coolant, grinding, space machinery, and boiler flue gas temperature reduction. They exhibit enhanced thermal conductivity and convective heat transfer coefficient counter balanced to the base fluid. Nanotechnology has enormous applications in industry. Fluids with nano-scaled particles interface are called nanofluid. The term nanofluid was proposed by Choi [27] Nanofluid heat transfer is a pioneering technology which can be used to augment heat transfer. Nanofluid is a deferral of solid nanoparticles (1–100nm diameters) inconventional liquids like water, oil, and ethylene glycol. The nano particles used in nanofluid are usually collected of metals, oxides, carbides, or carbon nanotubes. Water, ethylene glycol, and oil are familiar examples of base fluids. The effects of the wall thickness constraints are velocity power index, ratio of rates of velocities, radiation parameter and the Prandtl number on the membrane friction coefficient and the local Nusselt number, which represents the heat transfer rate at the surface, for the steady stagnation point flow and heat transfer towards stretching surface has been studied by Prasanna Kumara et al [28]

In current study we extended the work of Prasanna Kumara e.al [28], by taking into consideration the flow of an incompressible nanofluid stagnation point flow towards a stretching surface with variable thickness, thermal radiation. The fluid determined by a stretching surface located at $y = A(x+b)^{\frac{1-m}{2}}$ with a fixed stagnation point at x = 0.
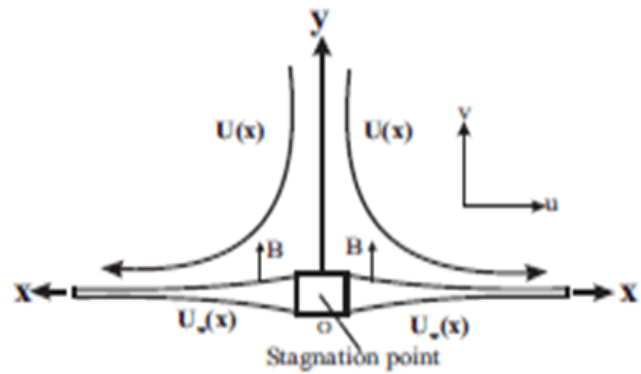

Figure 1: Schematic diagram of the flow

MATHEMATICAL ANALYSES

Consider the flow of an incompressible viscous fluid driven by a stretching surface located at $y = A(x+b)^{\frac{1-m}{2}}$ with a fixed stagnation point at $x = 0$ as shown in figure 1. We imagine that wall is impervious, non-flat with a given profile and the coefficient A being small so that the sheet is adequately thin. The stretching velocity $U_w(x)$ and the ambient fluid velocity $U(x)$ are assumed to be thickness of the stretched sheet from the stagnation point i.e., $U_w(x) = U_o(x+b)^m$ and $U(x) = U_1(x+b)^m$, where m is the velocity power index. Due to the acceleration or deceleration of the sheet, the thickness of the stretched sheet may decrease or increase with distance from the slot, which is reliant on the value of the velocity power index. With the above assumptions, the boundary layer equations prevailing the flow and temperature fields are given by,

$$\frac{\partial u}{\partial x} + \frac{\partial v}{\partial y} = 0, \tag{1}$$

$$\rho\left(u\frac{\partial u}{\partial x} + v\frac{\partial u}{\partial y}\right) = \mu\frac{\partial^2 u}{\partial y^2} - \frac{dp}{dx} - \frac{\sigma B_0^2}{\rho_f}u, \tag{2}$$

$$\rho c_p\left(u\frac{\partial T}{\partial x} + v\frac{\partial T}{\partial y}\right) = k\frac{\partial^2 T}{\partial y^2} - \frac{\partial q_r}{\partial y} + \tau\left[D_B\frac{\partial C}{\partial y}\frac{\partial T}{\partial y} + \frac{D_T}{T_\infty}\left(\frac{\partial T}{\partial y}\right)^2\right], \tag{3}$$

$$u\frac{\partial C}{\partial x} + v\frac{\partial C}{\partial y} = D_B\frac{\partial^2 C}{\partial y^2} + \frac{D_T}{T_\infty}\frac{\partial^2 T}{\partial y^2}, \tag{4}$$

Where u and v are the velocity components of the fluid along x and y directions respectively. M, μ, ρ, k and C_p are the magnetic parameter, the dynamic viscosity of the fluid, density of the fluid, thermal conductivity and specific heat of the fluid respectively. T is the temperature, T_∞ is stable temperature of the fluid in the in viscid free stream, α is the thermal conductivity, (ρc)p is the effective heat capacity of nanoparticles, (ρc)f is heat capacity of the base fluid, C is nanoparticle

volume fraction, D_B is the Brownian diffusion coefficient, and D_T is the thermophoretic diffusion coefficient. The allied boundary conditions for the present problem are

$$u = U_w(x), \ v = 0 \ ; T_w(x) = T_\infty + T_0(x + b)^{\frac{m}{2}};$$

$$C_w(x) = C_\infty + C_0(x + b)^{\frac{m}{2}}$$

$$at \ y = A(x + b)^{\frac{1-m}{2}} \tag{5}$$

$$u \to U(x) \ ; T \to T_\infty; \ C \to C_\infty \quad as \ y \to \infty \quad \text{where,} \ U_w 1(x) = U_0(x + b)^m$$
is the stretching velocity, U_0 and b are the physical parameter related with stretched surfaces. T_w and T_∞ denote the temperature at the wall and at large distance from the wall respectively and T_0 is the distinctive temperature. C_w is the variable wall nanoparticle volume fraction with C_0 being a constant and C_∞ is constant nanoparticle volume fraction in free stream, To employing the generalized Bernoulli's equation, in the free stream $U(x) = U_1(x + b)^m$ the equation (2) reduces to

$$U\frac{dU}{dx} = -\frac{1}{\rho}\frac{dp}{dx} \tag{6}$$

using (6) into (2) one can obtain

$$\rho\left(u\frac{\partial u}{\partial x} + v\frac{\partial u}{\partial y}\right) = \mu\frac{\partial^2 u}{\partial y^2} + U\frac{dU}{dx} \tag{7}$$

Using the Rossel and approximation for radiation, radiation heat flux is simplified as

$$q_r = -\frac{4\sigma^*}{3k^*}\frac{\partial T^4}{\partial y} \tag{8}$$

where σ^* and k^* are the Stefan-Boltzman constant and mean absorption co-efficient, respectively. Assuming that the temperature differences within the flow such that the term T^4 may be expressed as a linear function of the temperature, we expand T^4 in a Taylor series about T_∞ and neglecting the higher order terms beyond the first degree in $(T-T_\infty)$ we get

$$T^4 \cong 4T_\infty^3 T - 3T_\infty^4 \tag{9}$$

Substituting equations (8) and (9) in equation (3) reduces to

$$\rho c_p\left(u\frac{\partial T}{\partial x} + v\frac{\partial T}{\partial y}\right) = k\frac{\partial^2 T}{\partial y^2} - \frac{16\sigma^* T_\infty^3}{3k^*}\frac{\partial^2 T}{\partial y^2} \tag{10}$$

The momentum and energy equations can be transformed using the following correspondence renovation

$$\eta = \sqrt{\frac{(m+1)U_0}{2v}}\left[y(x+b)^{\frac{m-1}{2}} - A\right],$$

$$f = \frac{\psi}{\sqrt{\frac{2vU_0}{m+1}}(x+b^{m+1}f)} \tag{11}$$

$$\theta(\eta) = \frac{T-T_\infty}{T_w-T_\infty}, \ \varphi(\eta) = \frac{C-C_\infty}{C_w-C_\infty},$$

where η is the similarity variable and ψ is the stream function defined as $u = \frac{\partial\psi}{\partial y}$ and $v = -\frac{\partial\psi}{\partial x}$ which identically satisfies equations (1). Employing the similarity variables (11) equations (7) and (10) reduce to the following ordinary differential equations

$$f'''(\eta) + f(\eta)f''(\eta) + \frac{2m}{m+1}\left[\lambda^2 - f'^2(\eta)\right] - \frac{2}{m+1}Mf' = 0 \tag{12}$$

$$\left(1 + \frac{4}{3}Nr\right)\frac{1}{Pr}\theta''(\eta) + f(\eta)\theta'(\eta) - \frac{m}{m+1}f'(\eta)\theta(\eta) + Nb\theta'(\eta)\varphi'(\eta) + Nt\theta'^2(\eta) = 0 \tag{13}$$

$$\emptyset''(\eta) + Le\left(f(\eta)\varphi'(\eta) - f'(\eta)\varphi(\eta)\right) + \frac{Nt}{Nb}\theta''(\eta) = 0, \tag{14}$$

subject to the boundary conditions (5) which becomes

$$\begin{cases} f(\eta) = \beta\left(\frac{1-m}{1+m}\right), f'(\eta) = 1 & \\ \theta(\eta) = 1, \ \varphi(\eta) = 1 & at \quad \eta = 0, \\ f'(\eta) = \lambda, \ \theta(\eta) = 0, \ \varphi(\eta) = 0 & at \quad \eta \to \infty \end{cases} \tag{15}$$

In the above equations, prime denotes differentiation with respect to η and $\beta = A\sqrt{\frac{U_0(m+1)}{2v}}$ is the wall thickness parameter, m is the velocity power index, $\lambda = \frac{U_1}{U_0}$ is the ratio of rates of velocities, $Nr = \frac{4\sigma^* T_\infty^3}{kk^*}$ is the radiation parameter and $Pr = \frac{\mu c_p}{k}$ is the Prandtl number, $M = \frac{\sigma B_0^2}{\rho_f}$ is the magnetic parameter, $Le = v/D_B$ is the Lewis number. The dimensionless parameter Nb (Brownian motion parameter) and Nt (thermophoresis parameter) are defined as

$$Nb = D_B\frac{(\rho c)_p}{(\rho c)_f}\frac{(C_w-C_\infty)}{v}, \ Nt = \frac{D_T}{T_\infty}\frac{(\rho c)_p}{(\rho c)_f}\frac{(T_w-T_\infty)}{v},$$

Here Pr, Le, Nb, Nt, M, and Nr denote the Prandtl number, the Lewis number, the Brownian motion parameter, the thermophoresis parameter, magnetic parameter, Radiation parameter respectively. This boundary value problem is reduced to the classical problem of flow and heat and mass transfer due to a stretching surface in a viscous fluid when n = 1 and Nb = Nt = 0 in eqs (13) and (14).

The quantities of practical interest, in this study, are the local skin friction C_{fx} Nusselt number N_{ux} and the Sherwood number Sh_x which are defined as

$$C_{fx} = \frac{\mu_f}{\rho u_w^2}\left(\frac{\partial u}{\partial y}\right)_{y=0}, \ Nu_x = \frac{xq_w}{k(T_w - T_\infty)}, \ Sh_x = \frac{xq_m}{D_B(C_w - C_\infty)} \tag{16}$$

Where k is the thermal conductivity of the nanofluid, and q_w, q_m are the heat and mass fluxes at the surface, respectively, given by

$$q_w = -\left[\frac{\partial T}{\partial y}\right]_{y=0}, \ q_m = -D_B\left[\frac{\partial C}{\partial y}\right]_{y=0} \tag{17}$$

Substituting Eq (11) into Eqs (16) − (17), we obtain

$$\text{Re}_x^{1/2} C_{fx} = \sqrt{\frac{n+1}{2}} f''(0),$$

$$\text{Re}_x^{-1/2} Nu_x = -\sqrt{\frac{n+1}{2}} \theta'(0)$$

$$\text{Re}_x^{-1/2} Sh_x = -\sqrt{\frac{n+1}{2}} \varphi'(0)$$

Where $\text{Re}_x = u_w \dfrac{x}{v}$ is the local Reynolds number.

Table 1: Comparison of the values of membrane friction coefficient $f''(0)$ for a choice of values of m and for fixed values $\lambda = Pr = Nr = 0$ and $\beta = 0.5$

M	Fang et al.	Prasanna Kumar et al	Present results
10	-1.0603	-1.06034	-1.0602
7	-1.0550	-1.05506	-1.0549
3	-1.0359	-1.03588	-1.0358
1	-1.0000	-1.00000	-1.0000

Table 2: Result Values of skin friction $-f''(0)$, Nusslet number $-\theta'(0)$ and Sherwood number $-\varphi'(0)$ for different values of physical parameters

β	Pr	Nr	M	Nt	Nb	Le	λ	$-f''(0)$	$-\theta'(0)$	$-\varphi'(0)$
0.5	3	2	2	1	1	2	0.5	0.7022	0.4178	1.4140
1.0								0.6620	0.3933	1.2632
1.5								0.6241	0.3707	1.1254
0.5	1							0.7022	0.3481	1.4140
	2							0.7022	0.4043	1.4298
	3							0.7022	0.4178	1.4449
		2						0.7022	0.4178	1.4140
		2.5						0.7022	0.4144	1.4072
		3						0.7022	0.4091	1.4028
			1					0.6676	0.3990	1.6180
			2					0.7022	0.4178	1.4140
			4					0.7272	0.4340	1.2630
				1				0.7022	0.4178	1.4140
				2				0.7022	0.3501	1.4308
				3				0.7022	0.3040	1.4562
					0.5			0.7022	0.5146	1.2610
					1			0.7022	0.4178	1.4140
					1.5			0.7022	0.3405	1.4546
						1		0.7022	0.4574	0.9255
						2		0.7022	0.4178	1.4140
						3		0.7022	0.3979	1.7520
							0.2	0.9528	0.3874	1.3010
							1.5	0.9797	0.5176	1.7763
							2	2.1870	0.5629	1.9401

RESULTS AND DISCUSSION

The classification of equations (1)-(4) along with the boundary condition (5) has been solved numerically by using implied finite difference scheme known as Keller Box method.

The abridged Eqs. (12)–(15) are nonlinear and united, and thus their exact methodical solutions are not potential. They can be solved numerically using Keller – Box for dissimilar values of parameters such as magnetic parameter, Prandtl, Eckert and the Lewis numbers, the Brownian motion parameter and the thermophoresis parameter. The possessions of the emerging parameters on the dimensionless velocity, temperature, membrane friction, the rates of heat and mass transfer are investigated.

The important steps in using the Keller Box method are:

1) Tumbling higher order ODEs (systems of ODEs) in to system of first order ODEs;
2) Writing the systems of first order ODEs into difference equations using central differencing scheme;
3) Liberalizing the difference equations using Newton's method and writing it in vector form;
4) Solving the system of equations using block eliminations method.

In order to solve the above degree of difference equations numerically, we adopt Matlab software which is very efficient in using the well known Keller Box method.

In order to study precision of our results compared the present results with those of PrasannaKumaraet.al.,[28],when neglect the effects of Nt and Nb. The evaluation results ensures there is a good concurrence between the present and previous works Prasanna Kumara et al [28]. The computed results for some values of the prevailing flow parameters M,m, β, λ Nr, Nt, Nb ,Le are analyzed graphically for velocity, temperature and nanoparticle volume fraction profiles in figures (2) to (9).

Fig. 2(a-c) exhibits the effect of magnetic parameter on the velocity. It is empirical that the velocity profile of the fluid is inconsequentially reduced with increasing values of M. An increase in magnetic parameter M results in a strong diminution in velocity. This is due to the fact that magnetic field introduces a retarding body force which acts oblique to the direction of the applied magnetic field. This body force, known as the Lorentz force, decelerates the boundary layer flow and the boundary layer thickness decreases with increase in magnetic parameter. The authority of magnetic parameter M on the temperature and concentration profiles is clearly observed to be appreciably enhanced with increasing magnetic parameter. As the Lorentz force is a resistive force which opposes the fluid motion, so heat is produced and as a result, the thermal boundary layer thickness become thicker for stronger magnetic field.

Fig 3(a)-(c), represents the deviation of velocity, temperature and nanoparticle volume fraction for different values of m. It is found from fig 3(a) that the velocity profiles decrease with the increase of m in case of $\lambda < 1$ and increase the velocity profiles with increase of m in case of $\lambda > 1$. For a fixed value of $\lambda = 0.5$ the temperature and nanoparticle volume fraction increases with the increase of m is depicted from the figure. One can seen that if m= 1, the problem reduces to a flat sheet problem.

Fig 4(a)-(c), illustrates the deviation in the velocity, temperature and nanoparticle volume fraction, respectively, for the different values of β. From the figure it is apparent that if β increases the fluid velocity is increases for a fixed value of $\lambda < 1$ whereas the fluid velocity decrease with increase of β for the value of $(\lambda > 1)$. This is because for higher value of β the boundary layer becomes thicker. It can be experimental from the figure that the temperature profiles and nanoparticle volume fraction profiles increases with increase of β. It can be noticed that an increase in wall thickness parameter results, increases the profiles of temperature and nanoparticle volume fraction.

Fig 5(a)-(c), exhibits the ratio of frees tiring velocity parameter λ on velocity, temperature and nanoparticle volume fraction profile respectively. It is observed that there is a decrease in the velocity and nanoparticle volume fraction profiles is noticed with an increasing λ. It is originated that when the stretching velocity is less than the free string velocity i.e., $\lambda < 1$, the flow as a boundary layer structure actually means the straining motion near the stagnation region increases, so the acceleration of the exterior stream increases which leads to decrease in the width of the boundary layer with increase in λ. In case of $\lambda < 1$ i.e., the stretching velocity of the float up exceeds the free string velocity then overturned boundary layer structure is formed. For $\lambda = 1$ there is no boundary layer formation because the stretching velocity is equal to free string velocity. It is apparent from the figure that the boundary layer thickness decreases with an increase in λ.

Fig 6(a)-(b), predicts the influence of radiation parameter Nr on temperature and nanoparticle volume fraction profiles, respectively. The radiation parameter Nr defines the comparative contribution of conduction, heat transfer to thermal radiation transfer. It is evident that an increase in the radiation parameter results with an increase in temperature field. It is seen that the nano particle volume fraction profiles decreases with the increase of radiation parameter Nr. This is an agreement with physical fact the thermal boundary layer thickness increases with an increase in Nr.

Fig7(a)-(b), illustrates the dimensionless temperature and nanoparticle volume fraction profiles for diverse values of thermophoresis parameter Nt. It is found from fig 7(a) the temperature increases with increase in nanoparticle volume fraction Nt. It is observed from fig 7(b) that increasing the value of thermophoresis Nt leads to enhances the nanoparticle volume fraction profiles.

Fig 8(a)-(b), has been plotted to displayed the Brownian motion parameter Nb on temperature, nanoparticle volume fraction profiles, respectively. It illuminates that the temperature profile increases with an increasing Brownian motion parameter Nb. It is also noticed from 8(b) that the nanoparticle volume fraction profiles decrease of increase Brownian motion parameter Nb. The concentration boundary layer reduces with an increasing Nb.

Fig 9(a)-(b), depicts the effects of Lewis number Le on temperature field and nanoparticle volume fraction profiles respectively. It is seen that increasing values of Lewis number Le result decrease the temperature field along with thermal boundary layer thickness. It is also observed that the high end profiles are to decrease with increasing Le. Thus increasing Le results to decrease the diffusion, which finally yields into a decrease of nanoparticle volume fraction.
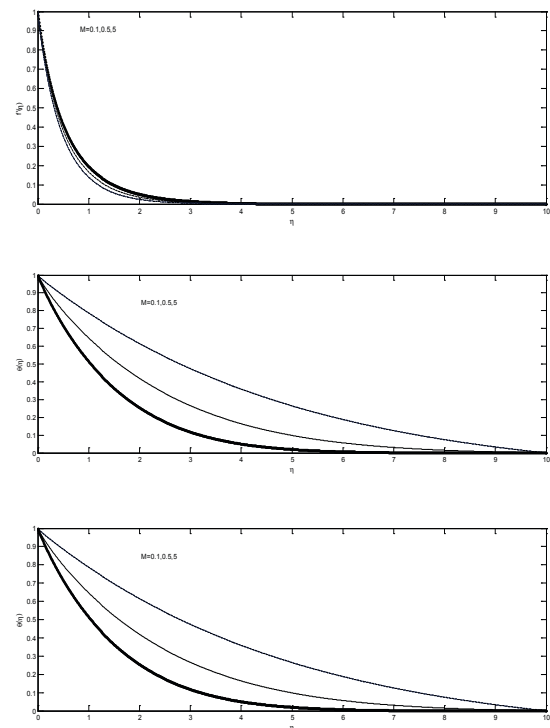

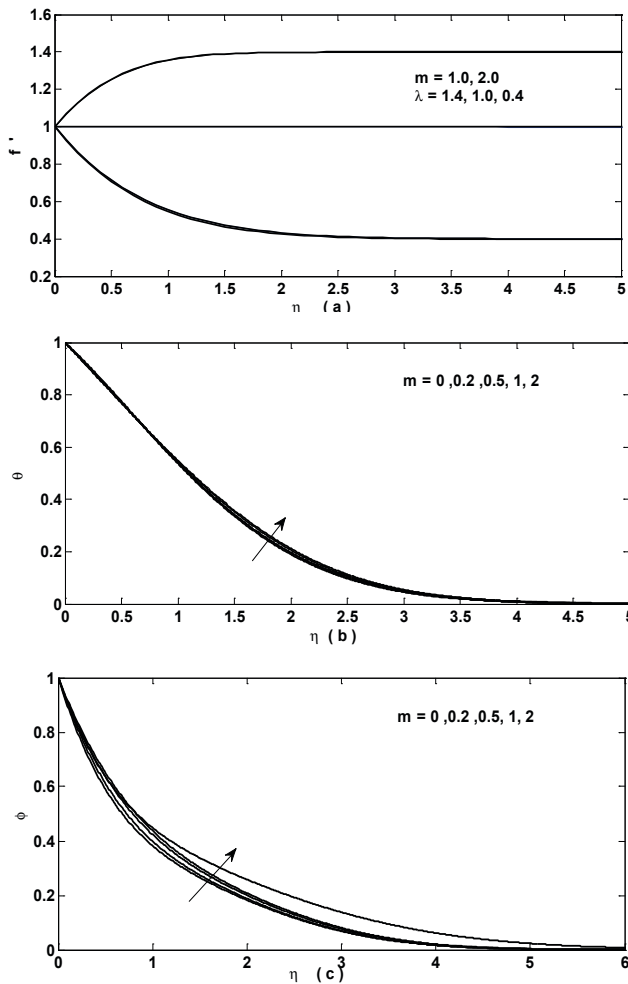**Figure 2:** Effects of M on Velocity, Temperature and Nanoparticle volume.

Figure 3: Effects of m on Velocity, Temperature and Nanoparticle volume.
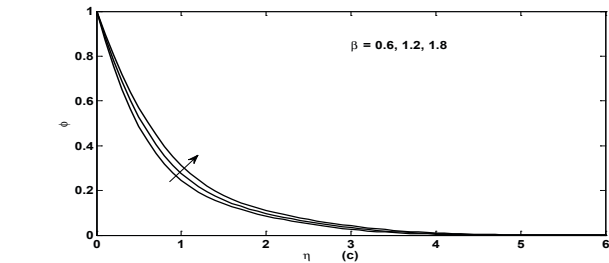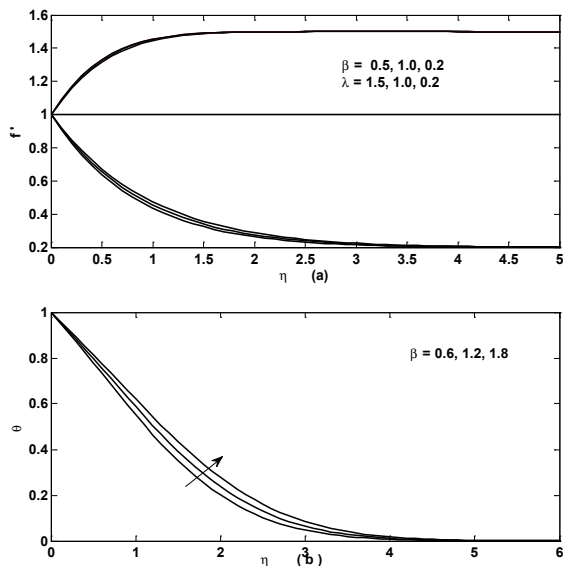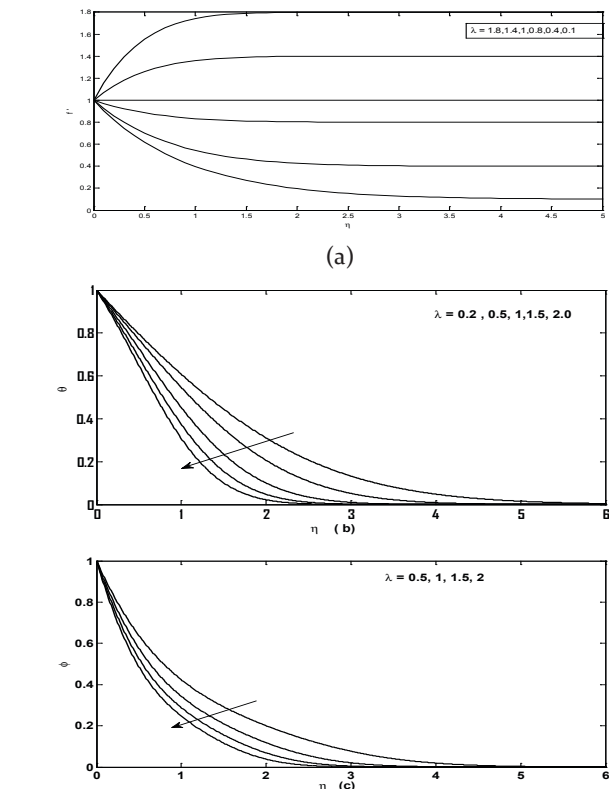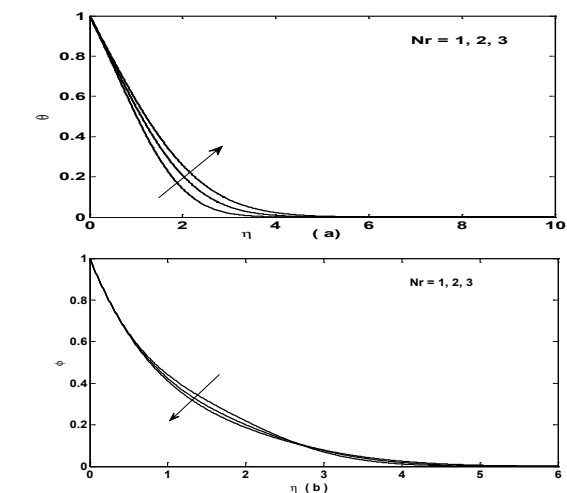

Figure 4: Effects of β on Velocity, Temperature and Nanoparticle volume.

Figure 5: Effects of λ on Velocity, Temperature and Nanoparticle volume.

Figure 6: Effects of Nr on Temperature and Nanoparticle volume.

Figure 7: Effects of Nt on Temperature and Nanoparticle volume.

Figure 8: Effects of Nb on temperature and Nanoparticle volume.

Figure 9: Effects of Le on Temperature and Nanoparticle volume.

CONCLUSION

The sturdy of two-dimensional boundary layer flow of an incompressible viscous nanofluid determined by a stretching surface with a fixed MHD stagnation point are present. The consequential partial differential equations are condensed to ordinary differential equations by using appropriate comparison transformations. The classification of ordinary differential equations are solved numerically by Keller Box method the numerical results obtainable to analyze the flow and heat transfer distinctiveness, Some of the imperative finding of four investigations are,

1. The effects of M, m and β leads to enhance the profiles of Temperature and Nanoparticle volume fraction, while the Magnetic parameter decreases velocity profile.
2. The stretching Velocity is less than the free stream velocity $\lambda > 1$. The flow as a boundary layer structure actually tells the straining motion near the stagnation region.
3. The stretching Velocity of the surface exceeds the free stream velocity $\lambda < 1$ transformed boundary layer structure is formed. For $\lambda = 1$ there is no boundary layer configuration. With the increase of λ, Temperature and Nanoparticle volume profiles decreases.
4. The effects of Radiation parameter (Nr) enhance the Temperature profiles and Nanoparticle volume fraction profiles.
5. The Temperature profiles and Nanoparticle volume fraction profiles increases with the effect of Thermophoresis parameter.
6. The augmentation of Brownian motion parameter is to develop the temperature profiles and reduce the Nanoparticle volume fraction.
7. The $f''(0)$ value decreases with increase of β and m. But there is no changes when increases the values of Nr, Nt, Pr changes. The $-\theta'(0)$ value decrease with increase in the values Nb, Nt, and Le.

ACKNOWLEDGEMENT

REFERENCES

1. K. Hiemenz, "The boundary layer on a circular cylinder in uniform flow (in German)", Dingl Polytech. J.326 (1911) 321-328.
2. T.C. Chiam, Stagnation point flow towards a stretching plate. J. Phys. Soc, Jpn, 63 (1994) 2443-2444.
3. Ishak A, Nazar R and Pop I " Mixed convection boundary layers in the stagnation-point flow toward a stretching vertical sheet", 2006 Meccanica 41 509.
4. Layek G C, Mukhopadhyay S and Samad S.K A ''Heat and mass transfer analysis for boundary layer stagnation-point flow
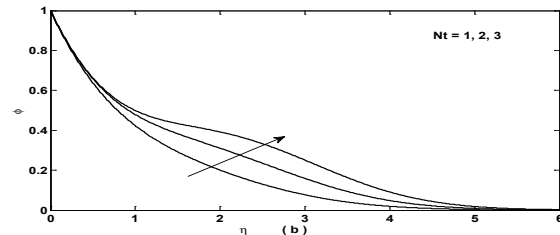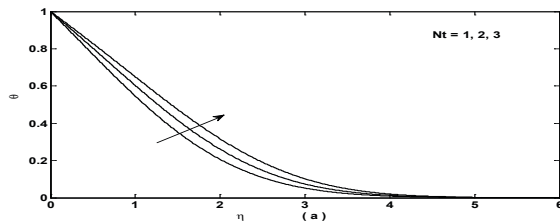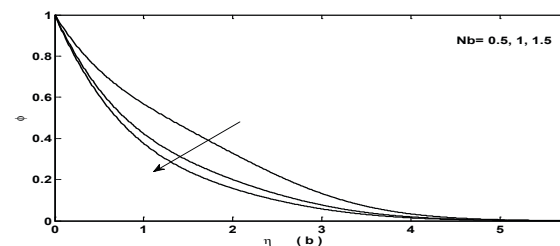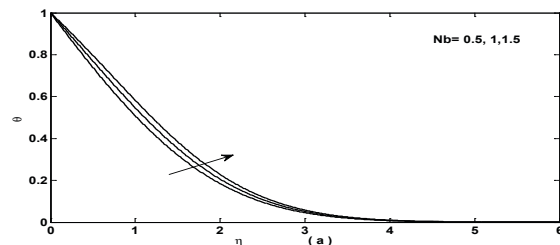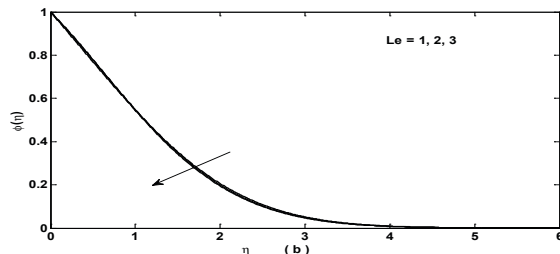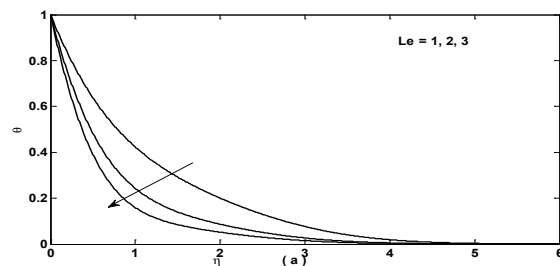
towards a heated porous stretching sheet with heat absorption/ generation and suction/blowing",2007 Int. Commun. Heat Mass Transfer 34 347.

5. Ding Q and Zhang H Q, "Heat transfer in boundary layer stagnation-point flow towards a shrinking sheet with non-uniform heat flux'', 2009 Chin. Phys. Lett. 26 104701.

6. M. Sheikholeslami, T. Hayat, A. Alsaedi MHD free convection of Al2O3–water nanofluid considering thermal radiation: a numerical study Int J Heat Mass Transf, 96 (2016), pp. 513-524.

7. M.M. Rashidi, S. Abelman, N. Freidooni Mehr Entropy generation in steady MHD flow due to a rotating porous disk in a nanofluid Int J Heat Mass Transf, 62 (0) (2013), pp. 515-525.

8. M. Sheikholeslami, M. Gorji-Bandpay, D.D. Ganji Magnetic field effects on natural convection around a horizontal circular cylinder inside a square enclosure filled with nanofluid Int Commun Heat Mass Transf, 39 (7) (2012), pp. 978-986.

9. M.M. Rashidi, M. Ali, N. Freidoonimehr, F. Nazari Parametric analysis and optimization of entropy generation in unsteady MHD flow over a stretching rotating disk using artificial neural network and particle swarm optimization algorithm Energy, 55 (15) (June 2013), pp. 497-510.

10. M. Sheikholeslami, M.M. Rashidi, T. Hayat, D.D. Ganji Free convection of magnetic nanofluid considering MFD viscosity effect J MolLiq, 218 (20P16), pp. 393-399.

11. S.A. Shehzad, Z. Abdullah, F.M. Abbasi, T. Hayat, A. Alsaedi-Magnetic field effect in three-dimensional flow of an Oldroyd-B nanofluid over a radiative surface J. Magn. Magn. Mater., 399 (2016), pp. 97-108.

12. Rizwan UlHaq, S. Nadeem, Z.H. Khan, N.F.M. NoorMHD squeezed flow of water functionalized metallic nanoparticles over a sensor surface Physica E: Low Dimen Syst Nanostruct (73) (2015), pp. 45-53.

13. O.D. Makinde, W.A. Khan, Z.H. Khan Buoyancy effects on MHD stagnation point flow and heat transfer of a nanofluid past a convectively heated stretching/shrinking sheet Int. J. Heat Mass Transf., 62 (2013), pp. 526-533.

14. Rizwan UlHaq, S. Nadeem, Z.H. Khan, N.F.M. Noor Convective heat transfer in MHD slip flow over a stretching surface in the presence of carbon nanotubes Physica B, 457 (15) (2015), pp. 40-47.

15. W.A. Khan, O.D. Makinde, Z.H. KhanNonaligned MHD stagnation point flow of variable viscosity nanofluids past a stretching

16. O.D. Makinde, F. Mabood, W.A. Khan, M.S. TshehlaMHD flow of a variable viscosity nanofluid over a radially stretching convective surface with radiative heat J. Mol. Liq., 219 (2016), pp. 624-630.

17. L.J. CraneFlow Past a Stretching Plate Zeitschriftfür Angewandte Mathematik und Physik (ZAMP), 21 (4) (1970), pp. 645-647

18. P. Carragher, L.J. CraneHeat transfer on a continuous stretching sheet ZAMM (1982), p. 62.

19. B.K. Dutta, P. Roy, A.S. GuptaTemperature field in flow over a stretching sheet with uniform heat flux Int Commun Heat Mass Transf, 12 (1985), p. 89.

20. J. Buongiorno Convective transport in nanofluids J Heat Transfer, 128 (3) (2010), pp. 240-250.

21. S. Kakac, A. Pramuanjaroenkij Review of convective heat transfer enhancement with nanofluids Int J Heat Mass Transfer, 52 (13) (2009), pp. 3187-3196.

22. S.E.B. Marga, S.J. Palm, C.T. Nguyen, G. Roy, N. GalanisHeat transfer enhancement by using nanofluids in forced convection flows Int J Heat Fluid Flow, 26 (4) (2005), pp. 530-546.

23. W.A. Khan, I. PopBoundary-layer flow of a nanofluid past a stretching sheet Int J Heat Mass Transfer, 53 (11) (2010), pp. 2477-2483.

24. A.V. Kuznetsov, D.A. NieldNatural convective boundary-layer flow of a nanofluid past a vertical plate Int J Therm Sci, 49 (2) (2010), pp. 243-247.

25. K. Vajravelu, K.V. Prasad, J. Lee, C. Lee, I. Pop, R.A.V. GorderConvective heat transfer in the flow of viscous Ag-water and Cu–water nanofluids over a stretching surface Int J Therm Sci, 50 (5) (2011), pp. 843-851.

26. N. Bachok, A. Ishak, L. Pop The boundary layers of an unsteady stagnation-point flow in a nanofluid Int J Heat Mass Transfer, 55 (22–23) (2012), pp. 6499-6505.

27. S.U. S. Choi, "Enhancing thermal conductivity of fluids with nanoparticles," in Proceedings of the ASME International Mechanical Engineering Congress and Exposition, vol. 66, pp.99–105, San Francisco, Calif, USA, November 1995.

28. B. C. Prasanna Kumara et al, MHD Stagnation Point Flow of Nanofluid Towards a Stretching Surface with Variable Thickness and Thermal Radiation /IJIM Vol. 7, No. 1 (2015) 77-85.